

On the static and small signal analysis of DAB converter

Yuxin Yang Hang Zhou Hourong Song Branislav Hredzak

Abstract—This document develops a method to solve the periodic operating point of Dual-Active-Bridge (DAB).

Index Terms—modal analysis, power electronics, Control theory.

I. INTRODUCTION

THE Dual-Active-Bridge is widely used for DC nano grid. In order to optimize the parameter design, a conversion ratio and a modal analysis are required. The traditional voltage & second balancing method is not applicable. Discrete time modeling method has been utilized to model the stability [1][2]. However, the complexity of existing discrete time model of DAB converter is too high for practical use. This paper derive a simplified discrete time model without sacrificing the accuracy. Therefore it is more practical for engineering use.

II. PROBLEM STATEMENT AND OBJECTIVES

We consider a piecewise linear time-invariant system over one period T_s , divided into n consecutive intervals of durations T_1, \dots, T_n (with $T_s = \sum_{i=1}^n T_i$). On interval i the system is governed by

$$\dot{\mathbf{X}}(t) = A_i \mathbf{X}(t) + B_i \mathbf{U},$$

where the input \mathbf{U} is held constant in each interval. Denote the state at the start of the i th interval by \mathbf{X}_{i-1} , then the discrete-time update is

$$\begin{aligned} \mathbf{X}_i &= \Phi_i \mathbf{X}_{i-1} + \Gamma_i, \quad \Phi_i = e^{A_i T_i}, \\ \Gamma_i &= \int_0^{T_i} e^{A_i(T_i-\tau)} B_i \mathbf{U} d\tau. \end{aligned} \quad (1)$$

Our goal is to derive:

- 1) A closed-form expression for \mathbf{X}_n in terms of \mathbf{X}_0 and the Γ_i .
- 2) The fixed-point equation for the periodic steady state \mathbf{X}^* satisfying $\mathbf{X}_n = \mathbf{X}_0 = \mathbf{X}^*$.

III. PRODUCT NOTATION: DIRECTION AND BOUNDARY

We introduce two notations for multiplying the transition matrices:

$$\prod_{j=a}^b \Phi_j := \Phi_a \Phi_{a+1} \cdots \Phi_b, \quad \prod_{j=a}^b \Phi_j := \Phi_b \Phi_{b-1} \cdots \Phi_a,$$

for $a \leq b$. In particular,

$$\prod_{j=a}^a \Phi_j = \prod_{j=a}^a \Phi_j = \Phi_a.$$

In our closed-form formula only the “reverse” product $\prod_{j=1}^n \Phi_j$ appears, avoiding any need for an empty-product convention.

IV. MAIN RESULTS: RECURSIVE CLOSED-FORM AND FIXED-POINT EQUATION

A. Recursive Closed-Form

For any $n \geq 1$, the state at the end of the n th interval is

$$\mathbf{X}_n = \left(\prod_{j=1}^n \Phi_j \right) \mathbf{X}_0 + \sum_{i=1}^{n-1} \left(\prod_{j=i+1}^n \Phi_j \right) \Gamma_i + \Gamma_n \quad (1)$$

B. Periodic Fixed-Point Equation

If a periodic steady state $\mathbf{X}^* = \mathbf{X}_0 = \mathbf{X}_n$ exists, it satisfies

$$(I - \Pi) \mathbf{X}^* = \sum_{i=1}^{n-1} \left(\prod_{j=i+1}^n \Phi_j \right) \Gamma_i + \Gamma_n, \quad \Pi := \prod_{j=1}^n \Phi_j. \quad (2)$$

Take four state transition as an example:

$$\begin{aligned} X_1 &= \Phi_1 X_0 + \Gamma_1, \\ X_2 &= \Phi_2 \Phi_1 X_0 + \Phi_2 \Gamma_1 + \Gamma_2, \\ X_3 &= \Phi_3 \Phi_2 \Phi_1 X_0 + \Phi_3 \Phi_2 \Gamma_1 + \Phi_3 \Gamma_2 + \Gamma_3, \\ X_4 &= \Phi_4 \Phi_3 \Phi_2 \Phi_1 X_0 + \Phi_4 \Phi_3 \Phi_2 \Gamma_1 + \Phi_4 \Phi_3 \Gamma_2 + \Phi_4 \Gamma_3 + \Gamma_4. \end{aligned} \quad (2)$$

V. SYSTEM MATRICES FOR DUAL ACTIVE BRIDGE

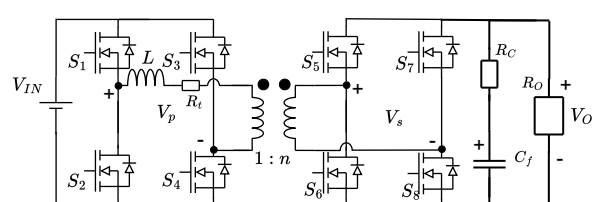


Fig. 1: Schematic of the DAB converter

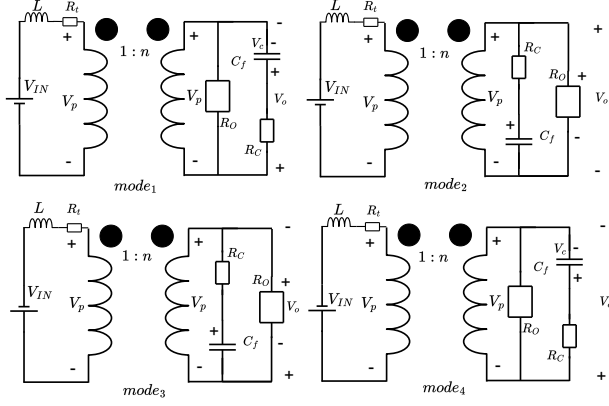


Fig. 2: Schematic of the piecewise intervals.

- 1) Subinterval T_1 : S_1, S_4, S_6, S_7 are ON; S_2, S_3, S_5, S_8 are OFF (A_1, B_1, C_1).
- 2) Subinterval T_2 : S_1, S_4, S_5, S_8 are ON; S_2, S_3, S_6, S_7 are OFF (A_2, B_2, C_2).
- 3) Subinterval T_3 : S_2, S_3, S_5, S_8 are ON; S_1, S_4, S_6, S_7 are OFF.
- 4) Subinterval T_4 : S_2, S_3, S_6, S_7 are ON; S_1, S_4, S_5, S_8 are OFF.

$$X = \begin{bmatrix} i_L \\ v_{CO} \end{bmatrix} \quad Y = [v_O] \quad U = [V_{IN}] \quad (3)$$

The output variable is :

$$\mathbf{y} = \begin{bmatrix} I_{rec} \\ V_{out} \end{bmatrix}$$

All matrices refer to the four-interval model ($n = 4$):

$$A_1 = A_4 = \begin{bmatrix} \frac{n^2 R_t + R_o R_C}{R_o + R_C} & \frac{R_o}{n L (R_o + R_C)} \\ -\frac{n^2 L}{R_o + R_C} & \frac{1}{C_o (R_o + R_C)} \end{bmatrix}$$

$$A_2 = A_3 = \begin{bmatrix} \frac{n^2 R_t + R_o R_C}{R_o + R_C} & \frac{R_o}{n L (R_o + R_C)} \\ -\frac{n^2 L}{R_o + R_C} & \frac{1}{C_o (R_o + R_C)} \end{bmatrix}$$

$$B_1 = B_2, \quad B_3 = B_4$$

$$B_1 = B_2 = \begin{bmatrix} 1 \\ \frac{1}{L} \end{bmatrix}, \quad B_3 = B_4 = \begin{bmatrix} -\frac{1}{L} \\ 0 \end{bmatrix}.$$

$$C_1 = \begin{bmatrix} -\frac{1}{n} & 0 \\ -\frac{1}{n} (R_C \parallel R_o) & \frac{R_o}{R_C + R_o} \end{bmatrix},$$

$$C_2 = \begin{bmatrix} \frac{1}{n} & 0 \\ \frac{1}{n} (R_C \parallel R_o) & \frac{R_o}{R_C + R_o} \end{bmatrix},$$

$$C_3 = C_2,$$

$$C_4 = C_1,$$

VI. NOTATION

$$S = \text{diag}(1, -1), \quad D' = \text{diag}(-1, 1), \quad SD' = -I.$$

For each subinterval $i = 1, \dots, 4$ let

$$\Phi_i = e^{A_i T_i}, \quad \Gamma_i = A_i^{-1} (\Phi_i - I) B_i U.$$

VII. SIMILARITY / SIGN IDENTITIES

$$\begin{aligned} A_2 &= A_3 = S A_1 S, & A_4 &= A_1, \\ B_1 &= B_2, & B_3 &= B_4 = -B_1, \\ T_1 &= T_3, & T_2 &= T_4. \end{aligned}$$

Lemma 1 (Similarity and Sign Relations). *Let*

$$\Phi_i = e^{A_i T_i}, \quad \Gamma_i = A_i^{-1} (\Phi_i - I) B_i U, \quad S = \text{diag}(1, -1),$$

with the structural and timing assumptions

$$\begin{aligned} A_2 &= A_3 = S A_1 S, & A_4 &= A_1, \\ B_1 &= B_2, \quad B_3 = B_4 = -B_1, & T_1 &= T_3, \quad T_2 = T_4. \end{aligned}$$

Then the following hold:

$$\Phi_3 = S \Phi_1 S, \quad \Phi_4 = S \Phi_2 S, \quad \Gamma_3 = -S \Gamma_1, \quad \Gamma_4 = -S \Gamma_2.$$

Proof. We verify each identity in turn, keeping every factor of S explicit.

1. $\Phi_3 = S \Phi_1 S$.

$$\begin{aligned} \Phi_3 &= e^{A_3 T_3} = e^{(S A_1 S) T_1} = S e^{A_1 T_1} S \\ &= S \Phi_1 S. \end{aligned} \quad (4)$$

2. $\Phi_4 = S \Phi_2 S$.

$$\Phi_4 = e^{A_4 T_4} = e^{A_1 T_2} = S e^{A_1 T_2} S = S \Phi_2 S. \quad (5)$$

3. $\Gamma_3 = -S \Gamma_1$.

$$\begin{aligned} \Gamma_3 &= A_3^{-1} (\Phi_3 - I) B_3 U \\ &= (S A_1 S)^{-1} (S \Phi_1 S - I) (-B_1) U \\ &= S A_1^{-1} S [S (\Phi_1 - I) S] (-B_1) U \\ &= -S [A_1^{-1} (\Phi_1 - I) B_1 U] = -S \Gamma_1. \end{aligned} \quad (6)$$

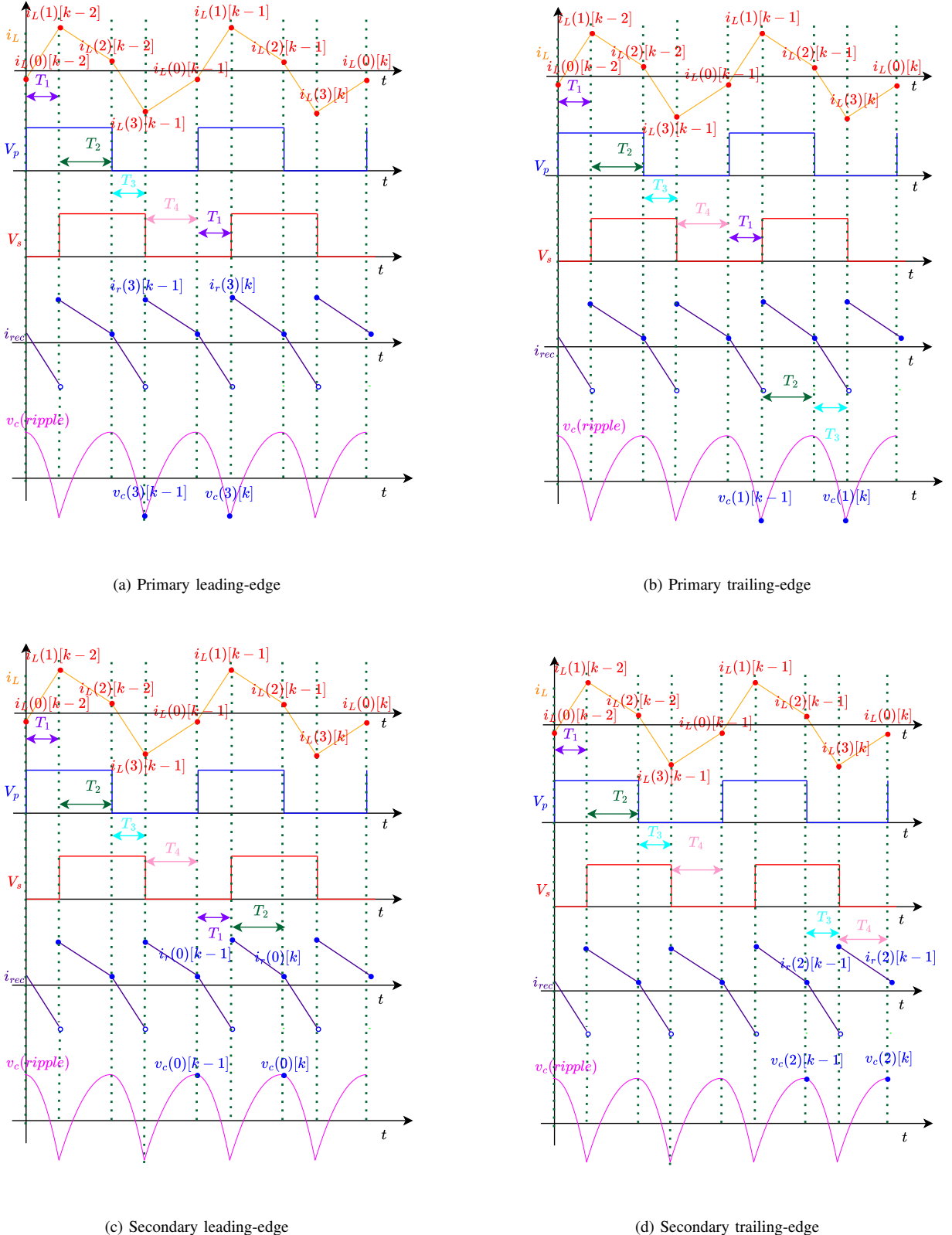


Fig. 3: Four modulation edges in DAB control.

$$4. \Gamma_4 = -S\Gamma_2.$$

$$\begin{aligned}
 \Gamma_4 &= A_4^{-1}(\Phi_4 - I)B_4U \\
 &= A_1^{-1}(\Phi_4 - I)(-B_1)U \\
 &= -A_1^{-1}(S\Phi_2S - I)B_1U \\
 &= -A_1^{-1}S(\Phi_2 - I)SB_1U
 \end{aligned} \tag{7}$$

This completes the proof of all four identities. \blacksquare

VIII. H - G OPERATOR PROOF FOR THE FOUR-STEP FIXED POINT

Theorem 2 (Half-Cycle Fixed-Point Characterization). *Under the symmetry assumptions*

$$S = \text{diag}(1, -1), \quad D' = \text{diag}(-1, 1),$$

$$SD' = -I, \quad T_1 = T_3, \quad T_2 = T_4,$$

$$A_2 = A_3 = S A_1 S,$$

$$A_4 = A_1, \quad B_3 = B_4 = -B_1,$$

let

$$\Phi_i = e^{A_i T_i}, \quad \Gamma_i = \int_0^{T_i} e^{A_i(T_i - \tau)} B_i U d\tau,$$

and define the half-cycle map

$$H(X) = \Phi_2 \Phi_1 X + (\Phi_2 \Gamma_1 + \Gamma_2).$$

Then the full-period fixed-point condition

$$\begin{aligned} X_4 &= \Phi_4 \Phi_3 \Phi_2 \Phi_1 X_0 + \Phi_4 \Phi_3 \Phi_2 \Gamma_1 \\ &+ \Phi_4 \Phi_3 \Gamma_2 + \Phi_4 \Gamma_3 + \Gamma_4 = X_0 \end{aligned} \quad (8)$$

is equivalent to the much shorter “half-cycle” condition

$$H(X_0) = D' X_0.$$

In other words, verifying

$$\Phi_2 \Phi_1 X_0 + (\Phi_2 \Gamma_1 + \Gamma_2) = D' X_0$$

alone guarantees $X_4 = X_0$, thereby reducing the four-step iteration to a two-step check.

Proof. Step1: Define Two Half-Cycle Maps

$$H(X) = \Phi_2 \Phi_1 X + \Phi_2 \Gamma_1 + \Gamma_2,$$

$$G(Z) = \Phi_4 \Phi_3 Z + \Phi_4 \Gamma_3 + \Gamma_4.$$

Step2: Two-Step Flip Condition

$$H(X_0) = D' X_0. \quad (H)$$

Step3: Structure of G

$$G(Z) = S \left[\Phi_2 \Phi_1 (S Z) - \Phi_2 \Gamma_1 - \Gamma_2 \right]. \quad (9)$$

Step4: Evaluate G at $Z = H(X_0)$

Because $SD' = -I$,

$$S H(X_0) = -X_0.$$

Insert into (9):

$$\begin{aligned} G(H(X_0)) &= S \left[\Phi_2 \Phi_1 (-X_0) - \Phi_2 \Gamma_1 - \Gamma_2 \right] \\ &= -S \left[\Phi_2 \Phi_1 X_0 + \Phi_2 \Gamma_1 + \Gamma_2 \right]. \end{aligned} \quad (10)$$

Step5: Apply Two-Step Condition Using (H),

$$\Phi_2 \Phi_1 X_0 + \Phi_2 \Gamma_1 + \Gamma_2 = D' X_0.$$

Substitute into (10):

$$G(H(X_0)) = -S D' X_0 = X_0.$$

Step6: Four-Step Closure Since $X_2 = H(X_0)$,

$$X_4 = G(X_2) = G(H(X_0)) = X_0.$$

IX. SMALL-SIGNAL MODEL OF DAB UNDER FIXED-FREQUENCY PHASE MODULATION

A. Half-cycle rectified coordinate and SIMO physical output

Consider the four-interval DAB model with state

$$x = \begin{bmatrix} i_L \\ v_C \end{bmatrix}, \quad (11)$$

and define the half-cycle length $T_h := T_s/2$. Following the rectification framework, we use a half-cycle rectified state (denoted with the same symbol for simplicity) by applying a fixed involution at each half-cycle boundary:

$$D_r := \text{diag}(-1, 1), \quad D_r^{-1} = D_r. \quad (12)$$

This choice makes the sampled inductor current sign-consistent across half-cycles.

We adopt a SIMO physical output

$$y = \begin{bmatrix} I_{\text{rec}} \\ V_{\text{out}} \end{bmatrix} = C_{\text{phys}} x, \quad (13)$$

where the constant matrix C_{phys} absorbs both the turns ratio factor and the output selection, so no C_{sel} is needed:

$$C_{\text{phys}} := \begin{bmatrix} \frac{1}{n} & 0 \\ \frac{R_c \parallel R_o}{n} & \frac{R_o}{R_c + R_o} \end{bmatrix}, \quad (14)$$

with $R_c \parallel R_o := \frac{R_c R_o}{R_c + R_o}$. Equation (14) provides a unified SIMO output for all half-cycle sampling surfaces considered below, up to a possible constant sign convention discussed in Section IX-E.

B. Segment maps, endpoint identity, and a two-interval half-cycle template

Pick any half-cycle sampling surface such that the half-cycle evolution consists of two consecutive subintervals $a \rightarrow b$ with durations T_a and T_b satisfying $T_a + T_b = T_h$. On subinterval $i \in \{a, b\}$ the dynamics are

$$\dot{x} = A_i x + B_i U, \quad (15)$$

and the exact segment map is

$$x^+ = \Phi_i x^- + \Gamma_i, \quad \Phi_i := e^{A_i T_i}, \quad \Gamma_i := \int_0^{T_i} e^{A_i(T_i - \tau)} B_i U d\tau. \quad (16)$$

1) A. Endpoint identity: A key identity for timing sensitivities is the endpoint vector-field form:

$$\frac{\partial}{\partial T} \left(\Phi(T) x^- + \Gamma(T) \right) = A x^+(T) + B U, \quad (17)$$

where $x^+(T) = \Phi(T) x^- + \Gamma(T)$ is the state at the end of the segment.

2) B. Large-signal half-cycle map: The rectified half-cycle map is

$$\begin{aligned} x_{k+1} &= D_r \left(\Phi_b \left(\Phi_a x_k + \Gamma_a \right) + \Gamma_b \right) \\ &=: \Phi^{(ab)} x_k + g^{(ab)}, \end{aligned} \quad (18)$$

where

$$\Phi^{(ab)} := D_r \Phi_b \Phi_a, \quad g^{(ab)} := D_r (\Phi_b \Gamma_a + \Gamma_b). \quad (19)$$

3) *C. Endpoint timing sensitivities*: Let x^* denote the fixed point of (18) for the chosen surface. Define the intermediate steady states along the half-cycle orbit:

$$\begin{aligned} x_{a,\text{end}}^* &= \Phi_a x^* + \Gamma_a, \\ x_{b,\text{end}}^* &= \Phi_b x_{a,\text{end}}^* + \Gamma_b. \end{aligned} \quad (20)$$

Using (17), the timing sensitivities of the rectified map (18) are

$$\begin{aligned} \eta_a^{(ab)} &:= \frac{\partial x_{k+1}}{\partial T_a} \Big|_* = D_r \Phi_b \left(A_a x_{a,\text{end}}^* + B_a U \right), \\ \eta_b^{(ab)} &:= \frac{\partial x_{k+1}}{\partial T_b} \Big|_* = D_r \left(A_b x_{b,\text{end}}^* + B_b U \right). \end{aligned} \quad (21)$$

C. Correct fixed-frequency modulation without a same-cycle constraint

1) *A. Ramp slope and timing polarity*: Let the ramp have amplitude V_r over the half-period T_h , so the slope is

$$S_e := \frac{V_r}{T_h} \quad [\text{V/s}]. \quad (22)$$

For a comparator-generated edge time T , we write the small-signal timing law as

$$\hat{T} = \sigma \frac{\hat{v}_c}{S_e}, \quad \sigma \in \{+1, -1\}, \quad (23)$$

where σ captures the modulator polarity at that edge.

2) *B. Two-cycle timing split*: A fixed-frequency modulator anchors one endpoint of a half-cycle segment to the clock and generates the other endpoint by a comparator. As a result, the two timing perturbations entering (21) naturally belong to two different cycles. We therefore write

$$\hat{T}_{a,k} = \sigma_a \frac{\hat{v}_{c,k}}{S_e}, \quad \hat{T}_{b,k} = \sigma_b \frac{\hat{v}_{c,k+1}}{S_e}, \quad (24)$$

where $(\sigma_a, \sigma_b) \in \{\pm 1\}^2$ is the polarity pair for the chosen sampling surface.

3) *C. Linearized half-cycle map*: Linearizing (18) and substituting (24) yield

$$\hat{x}_{k+1} = \Phi^{(ab)} \hat{x}_k + \beta_-^{(ab)} \hat{v}_{c,k} + \beta_+^{(ab)} \hat{v}_{c,k+1}, \quad (25)$$

where we absorb $1/S_e$ into two input vectors:

$$\beta_-^{(ab)} := \sigma_a \frac{\eta_a^{(ab)}}{S_e}, \quad \beta_+^{(ab)} := \sigma_b \frac{\eta_b^{(ab)}}{S_e}. \quad (26)$$

4) *D. SIMO transfer function*: Taking the z transform of (25) gives

$$\hat{X}(z) = (zI - \Phi^{(ab)})^{-1} (\beta_-^{(ab)} + z\beta_+^{(ab)}) \hat{V}_c(z), \quad (27)$$

hence the SIMO transfer function from \hat{v}_c to $y = [I_{\text{rec}}, V_{\text{out}}]^T$ is

$$H_{\text{fix}}^{(ab)}(z) = C_{\text{phys}}^{(ab)} (zI - \Phi^{(ab)})^{-1} (\beta_-^{(ab)} + z\beta_+^{(ab)}). \quad (28)$$

Here $C_{\text{phys}}^{(ab)}$ equals C_{phys} in (14) unless a constant sign convention is required to align the physical output definitions across sampling surfaces; see Section IX-E.

D. Four fixed-frequency phase-modulation surfaces

The four-interval DAB admits two natural half-cycle sampling surfaces for secondary-side modulation and two for primary-side modulation. Each surface yields a two-interval map of the form (18).

1) A. Secondary-side modulation:

- *Surface S+ (between subintervals 2 and 3)*: $(a, b) = (2, 3)$.
- *Surface S- (between subintervals 4 and 1)*: $(a, b) = (4, 1)$.

2) B. Primary-side modulation:

- *Surface P+ (between subintervals 1 and 2)*: $(a, b) = (1, 2)$.
- *Surface P- (between subintervals 3 and 4)*: $(a, b) = (3, 4)$.

For each surface, the corresponding polarity pair (σ_a, σ_b) in (24) is determined by the modulator polarity at the two endpoints (clocked edge versus comparator edge).

E. Equivalence of the four surfaces

We next show that the four modulation surfaces in Section IX-D yield equivalent z -domain models under the DAB symmetry identities.

1) A. Similarity invariance of the z -domain transfer:

Lemma 3 (Similarity invariance). *Let T be nonsingular and define*

$$\Phi' = T\Phi T^{-1}, \quad b' = Tb, \quad C' = CT^{-1}. \quad (29)$$

Then

$$C'(zI - \Phi')^{-1} b' = C(zI - \Phi)^{-1} b. \quad (30)$$

Proof. Using $(zI - T\Phi T^{-1})^{-1} = T(zI - \Phi)^{-1} T^{-1}$, one obtains

$$\begin{aligned} C'(zI - \Phi')^{-1} b' &= CT^{-1} \left(T(zI - \Phi)^{-1} T^{-1} \right) Tb \\ &= C(zI - \Phi)^{-1} b. \end{aligned} \quad (31)$$

■

2) *B. DAB symmetry-induced similarity relations*: Let $S = \text{diag}(1, -1)$ and recall the structural identities

$$\Phi_3 = S\Phi_1 S, \quad \Phi_4 = S\Phi_2 S, \quad D_r = -S, \quad (32)$$

which are satisfied by the secondary-side rectified half-cycle model.

For the primary-side surfaces P+ and P-, direct substitution gives

$$\begin{aligned} \Phi^{(34)} &= D_r \Phi_4 \Phi_3 = (-S)(S\Phi_2 S)(S\Phi_1 S) \\ &= S(D_r \Phi_2 \Phi_1) S = S \Phi^{(12)} S. \end{aligned} \quad (33)$$

Moreover, the combined input direction entering (28) obeys

$$(\beta_-^{(34)} + z\beta_+^{(34)}) = S(\beta_-^{(12)} + z\beta_+^{(12)}), \quad (34)$$

which follows from (21)–(21), (32), and the sign relations among (A_i, B_i) across symmetric subintervals.

3) C. Main equivalence theorem:

Theorem 4 (Equivalence of fixed-frequency surfaces). *Under (32) and the polarity consistency encoded in (24), the state-space triples*

$$\left(\Phi^{(ab)}, \beta_-^{(ab)} + z\beta_+^{(ab)}, C_{\text{phys}}^{(ab)} \right) \quad (35)$$

associated with the four surfaces are pairwise similar. In particular, for $P+$ and $P-$ one can choose $T = S$ and obtain

$$H_{\text{fix}}^{(34)}(z) = H_{\text{fix}}^{(12)}(z) \quad \text{with} \quad C_{\text{phys}}^{(34)} := C_{\text{phys}}^{(12)}S^{-1}. \quad (36)$$

The remaining equalities between secondary-side and primary-side surfaces follow by the same argument using the corresponding symmetry mapping.

Proof. Using (33)–(34) we have

$$\Phi^{(34)} = S\Phi^{(12)}S^{-1}, \quad \beta_-^{(34)} + z\beta_+^{(34)} = S(\beta_-^{(12)} + z\beta_+^{(12)}). \quad (37)$$

Choosing $C_{\text{phys}}^{(34)} := C_{\text{phys}}^{(12)}S^{-1}$ and invoking Lemma 3 yields (36). \blacksquare

Remark 1. If one enforces a single fixed C_{phys} for all surfaces, then the equivalence is exact for any output channel whose row C satisfies $CS^{-1} = C$ (e.g., the rectified current channel). For a channel that flips sign under S , the two transfer functions differ only by a constant factor -1 (identical magnitude; phase shifted by π).

F. A strong same-cycle constraint and why it is accurate at low frequency

Some simplified fixed-frequency derivations impose a same-cycle complement constraint within a selected half-cycle surface, effectively assuming that the two timing perturbations are equal and opposite within cycle k :

$$\hat{T}_{b,k} \approx -\hat{T}_{a,k}. \quad (38)$$

Under (38), the input depends only on $\hat{v}_{c,k}$ and the explicit z factor disappears.

1) A. *Constrained model:* Using (21) and the timing law (23), the constrained linearized map becomes

$$\hat{x}_{k+1} = \Phi^{(ab)}\hat{x}_k + \beta_{\text{sc}}^{(ab)}\hat{v}_{c,k}, \quad (39)$$

where

$$\beta_{\text{sc}}^{(ab)} := \sigma_a \frac{\eta_a^{(ab)}}{S_e} - \sigma_b \frac{\eta_b^{(ab)}}{S_e}. \quad (40)$$

Hence

$$H_{\text{sc}}^{(ab)}(z) = C_{\text{phys}}^{(ab)}(zI - \Phi^{(ab)})^{-1}\beta_{\text{sc}}^{(ab)}. \quad (41)$$

2) B. *Exact-constrained difference:* Comparing (28) and (41), one obtains

$$\begin{aligned} \Delta H^{(ab)}(z) &:= H_{\text{fix}}^{(ab)}(z) - H_{\text{sc}}^{(ab)}(z) \\ &= C_{\text{phys}}^{(ab)}(zI - \Phi^{(ab)})^{-1}(z-1)\beta_+^{(ab)}. \end{aligned} \quad (42)$$

For $z = e^{j\omega T_h}$, $|z-1| = 2|\sin(\omega T_h/2)|$, and thus

$$|z-1| \leq \omega T_h, \quad \omega T_h \ll 1. \quad (43)$$

Assuming $\Phi^{(ab)}$ is stable and has no eigenvalue close to 1, $(zI - \Phi^{(ab)})^{-1}$ remains bounded near $z \approx 1$. Consequently, the constrained model is accurate at low frequency with a first-order error:

$$\|\Delta H^{(ab)}(e^{j\omega T_h})\| = O(\omega T_h), \quad \omega \rightarrow 0. \quad (44)$$

Remark 2. Equation (42) shows that the discrepancy is shaped by a discrete difference factor $(z-1)$. This explains why the constrained and the correct fixed-frequency models can exhibit nearly indistinguishable Bode plots over a wide low-frequency range, even though the exact model contains an intrinsic two-cycle z factor.

REFERENCES

- [1] A. Tong, L. Hang, H. S.-H. Chung, and G. Li, “Using sampled-data modeling method to derive equivalent circuit and linearized control method for dual-active-bridge converter,” *IEEE Journal of Emerging and Selected Topics in Power Electronics*, vol. 9, no. 2, pp. 1361–1374, 2021.
- [2] L. Shi, W. Lei, Z. Li, J. Huang, Y. Cui, and Y. Wang, “Bilinear discrete-time modeling and stability analysis of the digitally controlled dual active bridge converter,” *IEEE Transactions on Power Electronics*, vol. 32, no. 11, pp. 8787–8799, 2017.